BUBBLE ERUPTION PATTERNS AND GAS DYNAMICS IN THE FREEBOARD OF A GAS-FLUIDIZED BED: A DISCRETE ELEMENT MODEL (DEM) STUDY

J. R. Third and C. R. Müller
muelchri@ethz.ch
Institute of Energy Technology, Department of Mechanical and Process Engineering, ETH Zurich, Leonhardstrasse 27, 8092 Zurich, Switzerland.

Abstract
In this study the eruption patterns of a continuous stream of bubbles were simulated using the Discrete Element Model (DEM). The dimensions of the simulated bed were 532.8 × 200.1 × 9.6 mm and the fluidized particles had a diameter d_p =1.2 mm and density ρ_p = 2600 kg/m^3. In total 250000 particles were simulated. The bubble eruption patterns and profiles of the gas velocity in the freeboard obtained from the numerical simulations were compared to the experimental Particle Image Velocimetry (PIV) and acetone planar laser induced fluorescence (PLIF) measurements of Müller *et al*. [11]. In the DEM simulations the velocity of the gas leaving an erupting bubble was homogeneously distributed along the bubble dome. The time-averaged gas velocity profile revealed that, in the freeboard, the lowest velocity in the vertical direction was in the centre of the bed, whereas the highest was in vicinity to the walls.

Introduction
Gas-fluidized beds are widely used in industry, *e.g.* in catalytic cracking, granulation, drying of agricultural goods, or the gasification and combustion of coal and biomass. However, despite their widespread use in industry, various fluid-dynamic phenomena that occur in gas-fluidized beds, such as the formation, coalescence, splitting and eruption of bubbles, are still poorly understood. The eruption of bubbles at the surface of the bed and the subsequent mixing of the gas which originated from the erupting bubble with the gas in the freeboard is of particular importance for gasification and combustions processes using low-rank coal or biomass. For these fuels a considerable proportion of their total carbon content is released as volatile matter [1]. Due to insufficient gas exchange between the bubble and particulate phases, volatiles contained in bubbles do not react completely within the bed. Thus, a considerable portion of the released volatile matter reacts *via* homogeneous combustion in the freeboard of the bed. Consequently, the gas mixing in the freeboard, induced by the eruption of bubbles, can often be the rate limiting step. The situation is further complicated if biomass is fed from the top. Owing to their small density, biomass particles tend to float on the surface of the bed resulting in an almost complete release of un-combusted volatiles into the freeboard [2]. So far, most studies dealing with bubble eruption have concentrated on the entrainment and elutriation of the fluidized particles [3-5], whereas investigations concerning the gas phase dynamics are comparatively sparse. Currently, there exist three main models describing the bubble eruption and subsequent disturbance of the gas phase in the freeboard. The pulsed jet theory, proposed by Zenz and Weil [6] assumes that the bubbles that erupt at the surface behave like intermittent jets. Consequently, a highly irregular profile of the gas velocity across the column diameter would be expected. Later, based on measurements of the dynamics of bubbles erupting at the top of a fluidized bed, Pemperton and Davidson [7] proposed the so-called ghost bubble theory. In this model, it is assumed that, after eruption, the bubble retains its shape, forming a "ghost bubble". The third eruption model has been

proposed initially by Levy and Lockwood [8]. Here, the ejected particles reverse their flow direction and fall back into the bed, the drag force of these falling particles is sufficient to cause a reversal of the flow of the surrounding gas. This downward gas flow induces the formation of a toroidal vortex, which moves initially towards the walls. Subsequently, the vortex is carried upwards with the main flow in the fluidized bed. Using particle image velocimetry (PIV) and acetone-planar laser induced fluorescence (PLIF) measurements, Solimene *et al*. [9], Yorquez-Ramirez and Duursma [10] and Müller *et al*. [11] confirmed the formation of a toroidal vortex, however different mechanisms of gas release during the eruption process were reported. For example, Solimene *et al.* [9] observed the formation of a ‘‘nose pocket’’ of gas which is released at the center of the dome. The modified Levy and Lockwood [8] model, proposed by Solimene *et al*. [9] is shown in Fig.1: the main difference between the models of Levy and Lockwood [8] and Solimene *et al*. [9] is the formation of a nose pocket. However, subsequent Acetone-PLIF measurements by Hartung *et al*. [12] reported that the release of acetone during bubble eruption can occur in 5 different patterns, ranging from the formation of a nose-pocket, over a homogeneous release of acetone along the entire dome surface, to the majority of the acetone being released at the sides of the erupting dome. The different release patterns were attributed to the inhomogeneity of the thickness of the dome during bubble eruption. Yorquez-Ramirez and Duursma [10] confirmed the existence of different acetone release patterns, proposing an evenly distributed release of gas along the dome upon bubble eruption.

With respect to the flow velocity profile in the freeboard, Levy and Lockwood [8] were the first to report that the maxima of the gas velocities were found near the walls and not in the centre of the bed. More recently, PIV has been applied to image the flow pattern in the freeboard above an erupting bubble [11,13]. In agreement with earlier investigations, it was found that the maxima of the gas velocities were located near the walls. In contrast, the velocity in the centre of the freeboard was, depending on vertical position in the freeboard, negative or close to zero.

The objective of this study is to investigate for the first time the gas dynamics in the free board of a gas-fluidized bed using the discrete element model (DEM). The simulation results are compared with the experimental measurements of Müller *et al.* [11]. However, owing to the large number of particles in the system used by Müller *et al*. [11], it was not possible to simulate exactly the experimental set-up. The fluidized bed simulated was modified to reduce the number of particles to a manageable magnitude. Thus, only a qualitative comparison between the experimental and numerical results is possible.

Numerical

The simulations reported in this work were performed using a two-phase discrete element model based on the work of Tsuji *et al.* [14]. This method combines a discrete description of the solid phase [15] with the volume-averaged description of the fluid-phase derived by Anderson and Jackson [16]. The interaction between the fluid and particle phases is modelled using a momentum exchange coefficient, β, such that the motion of the particles is governed by:

$$m_p \frac{d\mathbf{v_p}}{dt} = -V_p \nabla p + \frac{V_p \beta}{(1-\varepsilon)}\left(\mathbf{u} - \mathbf{v_p}\right) + m_p \mathbf{g} + \mathbf{F}_c \qquad (1)$$

$$I_p \frac{d\boldsymbol{\omega}_p}{dt} = \mathbf{L}_c \qquad (2)$$

where m_p, I_p, $\mathbf{v}_p$, $\boldsymbol{\omega}_p$, V_p, $\mathbf{u}$, p, $\mathbf{F}_c$, $\mathbf{L}_c$, $\mathbf{g}$, and ε are, respectively, the mass, moment of inertia, translational velocity, rotational velocity, and volume of the particle; the velocity and pressure of the gas; the net force and torque acting on the particle due to collisions; the acceleration

due to gravity; and the voidage. The forces due to collisions are modelled using damped, linear springs and the force in the tangential direction is limited by Coulomb's law. The volume-averaged Navier-Stokes equations are:

$$\frac{\partial(\varepsilon\rho_f)}{\partial t} + \nabla\cdot(\varepsilon\rho_f\mathbf{u}) = 0 \qquad (3)$$

$$\frac{\partial(\varepsilon\rho_f\mathbf{u})}{\partial t} + \nabla\cdot(\varepsilon\rho_f\mathbf{uu}) = -\varepsilon\nabla p - \nabla\cdot(\varepsilon\boldsymbol{\tau_f}) - \mathbf{F}_p + \varepsilon\rho_f\boldsymbol{g} \qquad (4)$$

where $\boldsymbol{\tau}_f$ is the viscous stress tensor, $\mathbf{F}_p$ is the rate of exchange of momentum between the particulate and fluid phases and ρ_f is the density of the fluid phase. The fluid was assumed to be Newtonian; thus, the viscous stress tensor is given by:

$$\boldsymbol{\tau}_f = -\left(\lambda_f - \frac{2}{3}\mu\right)(\nabla\cdot\mathbf{u})\mathbf{I} - \mu\left((\nabla\mathbf{u}) + (\nabla\mathbf{u})^T\right) \qquad (5)$$

where λ_f and μ are the bulk and shear viscosity of the fluid and $\mathbf{I}$ is the identity matrix. The momentum exchange between the fluid and particulate phases is calculated by adding up the fluid forces acting on the individual particles in a fluid cell:

$$\mathbf{F}_p = \frac{1}{V_{cell}}\sum_{n=1}^{n=N_p}\frac{V_p\beta}{(1-\varepsilon)}\left(\mathbf{u}-\mathbf{v}_p\right) \qquad (6)$$

where V_{cell} is the volume of a fluid cell. The momentum exchange coefficient was calculated using the correlation proposed by Beetstra *et al.* [17].

The spatially averaged continuity and momentum equations for the gas phase were solved using an approach based on the SIMPLE algorithm and the equations of motion of the particles were integrated using a third-order Adams-Bashforth scheme. Table 1 summarises the parameter values used for the simulations reported here.

Table 1. Parameters values used for the simulation.

Bed	
Width	200.1 mm
Height	532.8 mm
Thickness	9.6 mm
Orifice width	9.84 mm
Particles	
Number	250000
Diameter	1.2 mm
Density	2600 kg/m^3
Normal stiffness	1000 N/m
Tangential stiffness	500 N/m
Coefficient of normal restitution	0.94
Coefficient of friction	0.3
Fluid	
Temperature	298.15 K
Viscosity	1.8×10^{-5} kg/(m s)
Molecular weight	28 kg/kmol
Cells in *x*-direction	61
Cells in *y*-direction	148
Cells in *z*-direction	1

The following system was studied numerically. At the bottom of the fluidized bed, gas of minimum fluidization velocity entered the bed homogeneously. Once the bed was incipiently fluidized, a separate flow of gas through the central orifice was specified.

Experimental

The fluidized bed used by Müller *et al*. [11] was of square cross-section with side length 200 mm. The distributor consisted of a perforated aluminium plate of 1.5 mm thickness, containing 81 holes, each of 0.5 mm dia. oriented in a square array. Such a distributor is expected to provide a very homogenous gas inlet, similar to a porous plate. Glass ballotini of size 150 – 250 μm were fluidized by air. Single bubbles or a stream of bubbles were injected into the incipiently fluidized bed *via* a nozzle of 10 mm i.d. The bed height at incipient fluidization was 250 mm. Assuming a bed voidage of 0.4 at incipient fluidization, the number of particles in the experimental set-up of Müller *et al*. [11] was ~ 1.6×10^9, which is roughly 3-4 orders of magnitude more than what could be simulated reasonably using the DEM.

Results

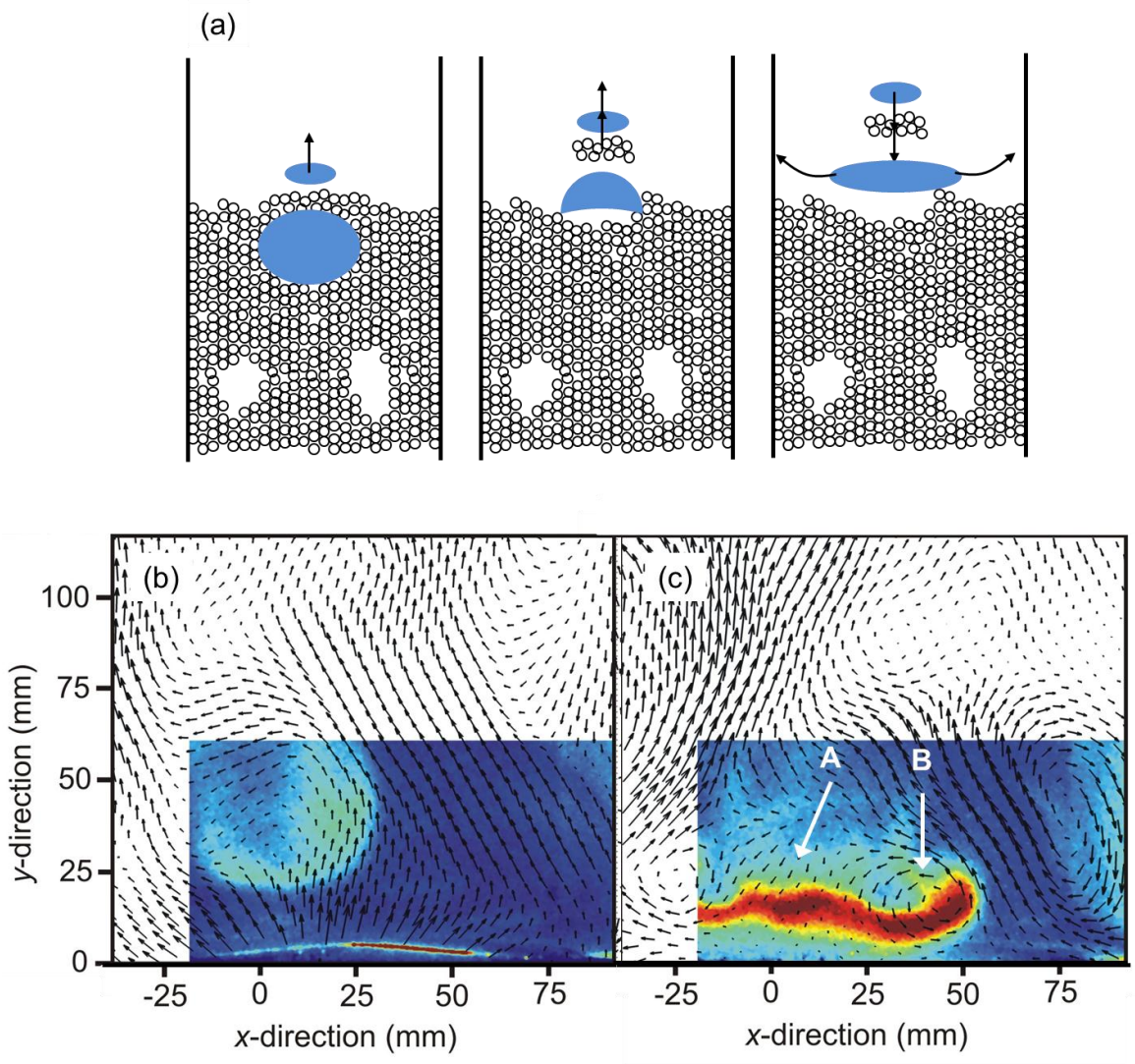

Figure 1. (a) Bubble eruption model proposed by Solimene *et al*. [9], (b,c) Simultaneous PIV (vector) and PLIF (color) measurements showing two different stages of bubble eruption patterns of single bubbles injected into an incipiently fluidized bed.

To aid the comparison between the experimental and numerical results, we first present the main results of the experimental study of Müller *et. al.* [11]. Figures 1(b,c) show snapshots of simultaneous PIV and acetone-PLIF measurements at two different stages of the eruption process of a stream of bubbles formed at the orifice. The vectors represent the gas velocity and the colour gives the acetone concentration. The fluidized bed was held at minimum fluidization. In Fig. 1(b) the early stage of a bubble eruption event is shown. Here, the acetone originally present in the erupting bubble is released almost homogenously throughout the bubble dome. This was one of five possible acetone release pattern reported by Hartung *et al*. [12]. The velocity of the gas at the top of the bubble dome is fairly constant along the bubble dome and directed radially into the freeboard. On the other hand, Fig. 1(c) shows the gas

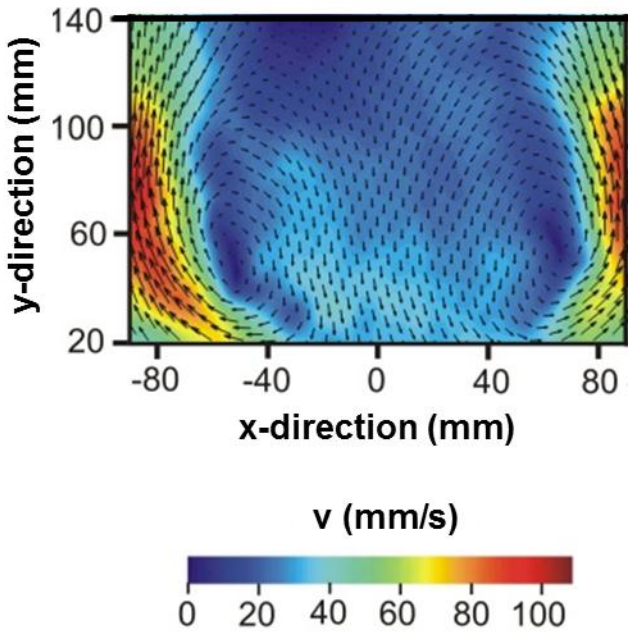

Figure 2. Time-averaged velocity profile of the gas flow in the freeboard for a continuous stream of bubbles: The vectors indicate the direction of the flow, whereas the color represents the magnitude of the velocity. The flow rate through the orifice was 71 cc/s, corresponding to an orifice velocity of U_0 = 0.90 m/s.

velocity profile and the acetone concentration towards the end of a bubble eruption event. Here, the dome is already collapsing, *i.e*. the particle velocity is directed downwards. The downwards moving particles induce a downwards motion of the gas phase, labeled "A", and induces the formation of a toroidal vortex wall just above the surface of the fluidized bed, labeled "B". This vortex is initially carried horizontally towards the walls. In a vertical cross-section, as shown here, the toroidal vortex appears as two vortex rings at the left and right of the erupting bubble. The left and right vortices rotate clockwise and anti-clockwise, respectively. Subsequently, the vortex is carried upwards with the main flow of the fluidized bed. The vorticity of the vortex decreases during the transport in the vertical direction.

Figure 2 shows the time averaged gas velocity profiles in the freeboard. The vectors indicate the direction of the flow, whereas the colour represents the magnitude of the velocity. The averaging time was ~ 30 s and the flow rate through the orifice was 71 cc/s, corresponding to an orifice velocity of U_0 = 0.90 m/s. Interestingly, and somewhat counter-intuitively, the time averaged velocity is directed downwards in the centre of the fluidized bed, whereas the velocity is upwards at the walls only. Consequently, there is also a strong

horizontal motion toward the walls in the vicinity of the surface of the fluidized bed. Müller *et al.* [11] reported that increasing the orifice velocity from 0.6 m/s to 1.1 m/s resulted in a small

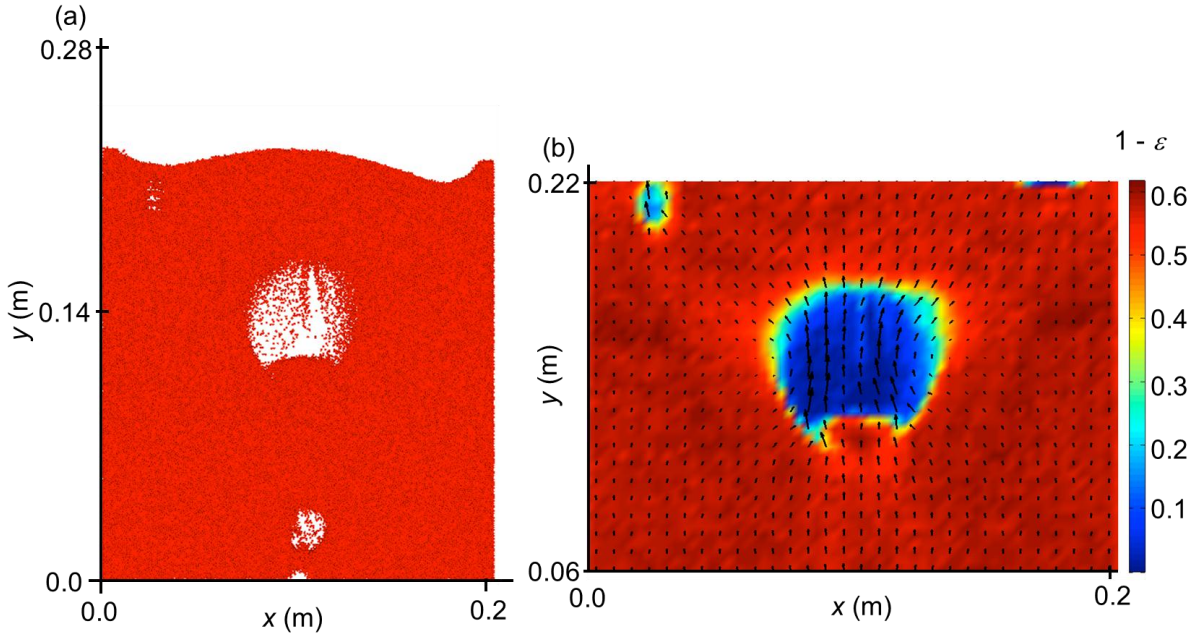

Figure 3. Typical snap-shot of a DEM simulation showing both the instantaneous particle distribution and the corresponding gas velocity pattern around a rising bubble. The bed was held at minimum fluidization velocity and the orifice velocity was U_0 = 5.64 m/s: (a) Instantaneous particle distribution and (b) vectors show the superficial gas velocity, the colour represents the solid fraction.

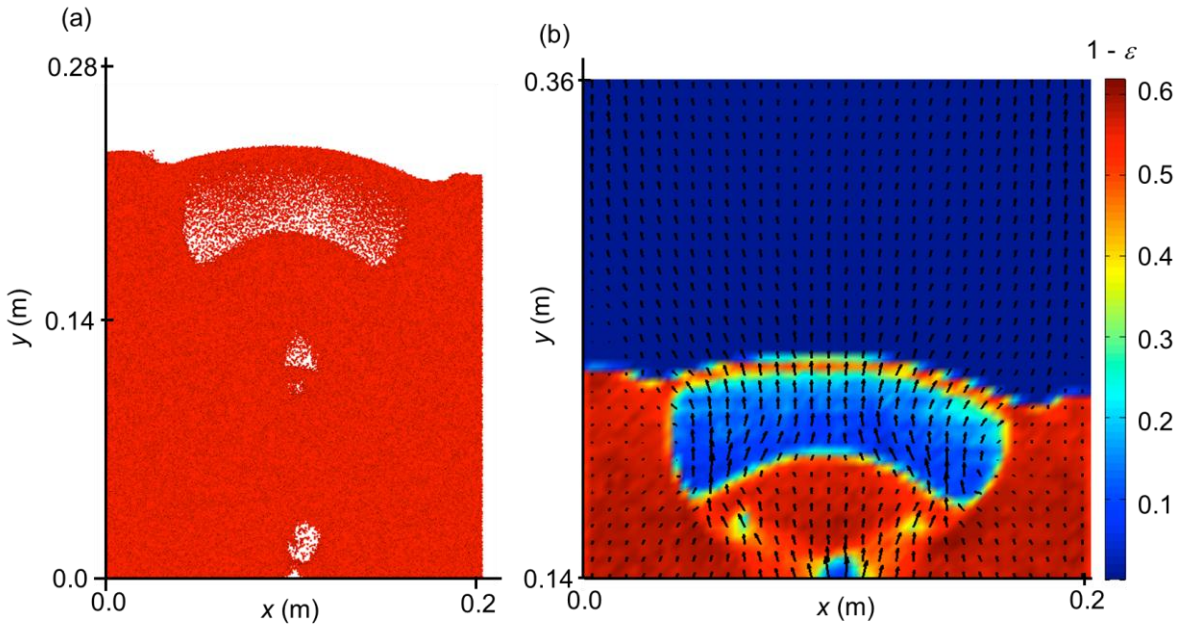

Figure 4. Typical snap-shot of a DEM simulation showing both the instantaneous particle distribution and the corresponding gas velocity pattern around an erupting bubble. The bed was held at minimum fluidization velocity and the orifice velocity was U_0 = 5.64 m/s: (a) Instantaneous particle distribution and (b) vectors show the superficial gas velocity, the colour represents the solid fraction.

increase in upward and downward velocities near the walls and the centre of the freeboard, respectively.

Turning now to the results of the DEM simulations. A typical snap-shot of the instantaneous particle distribution and gas velocity for a simulation with an orifice velocity of U_0 = 5.64 m/s is shown in Figs. 3(a) and (b), respectively. The bed was held at minimum fluidization. Figure 3(a) shows the rise of a single bubble through the fluidized bed. At the same time a new bubble forms at the orifice. In Fig. 3(b) the corresponding superficial gas velocity is shown as vectors, while the colour represents the solid fraction. The velocity vectors representing the flow of gas around and through the rising bubble show that the gas uses the bubble as a low-pressure drop short cut. A snap-shot of the instantaneous particle distribution of an erupting bubble and the corresponding flow field of the gas are shown in Figs. 4(a) and (b), respectively. In Fig. 4(b) the vectors represent the superficial gas velocity, whereas the colour corresponds to the solid fraction. Figure 4(a) shows clearly that the erupting bubble strongly increases its horizontal dimension during bubble eruption. This behaviour can also be observed experimentally in 2D beds of similar geometric dimensions. However, it is somewhat doubtful whether bubbles expand horizontally to the same extent in a 3D fluidized bed. From Fig. 4(b) it can be seen that gas velocity is (i) fairly constant along the dome of the erupting bubble and (ii) directed radially into the freeboard. Keeping the differences in the set-up of the systems for the numerical simulations and the experimental measurements in mind, the gas velocity profile shown in Fig. 4(b) shows qualitative good

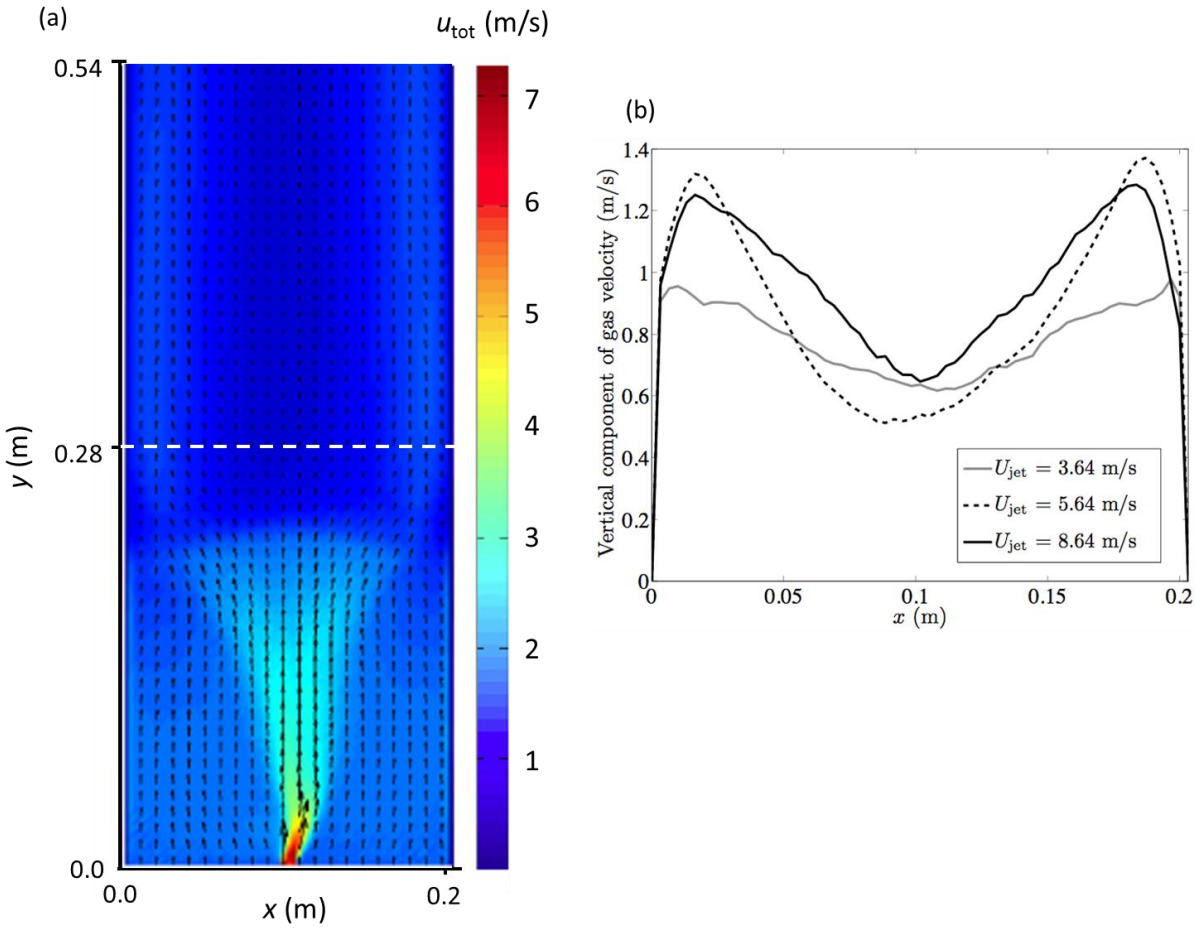

Figure 5. (a) Time-averaged interstitial gas velocity for U_0 = 5.64 m/s (b) Plots of the vertical velocity versus horizontal position for different orifice velocities at y = 0.28 m.

agreement with the profile shown in Fig. 1(a). However, it has to be mentioned that, unlike in the experimental measurements, in the numerical simulations no toroidal vortex was observed in the freeboard.

Figure 5(a) shows the time-averaged gas-velocity in the fluidized bed for an orifice velocity of U_0 = 5.64 m/s. In Fig. 5(a) the vectors indicate the direction of the flow, whereas the colour represents the vertical component of the interstitial velocity. Within the bed, *i.e.* $y <$ 0.23 m for U_0 = 5.64 m/s, the highest gas velocities can be found in the centre of the bed. However, in the freeboard, *i.e.* $y >$ 0.23 for U_0 = 5.65 m/s, the behaviour reverses, i.e. the gas velocity is smallest in the centre and highest in vicinity of the walls. This rather intriguing flow characteristic is maintained throughout the entire freeboard, albeit the differences between the gas velocities in the centre and close the walls decrease with height. Similar to the time-averaged PIV measurements, a horizontal velocity component directed towards the walls can be observed close to the top of the bed. The vertical velocity component as a function of horizontal position at y = 0.28 m is plotted in Fig. 5(b) for all three orifices velocities investigated.

Fig. 5(b) shows that increasing the velocity of the jet from 3.64 m/s to 5.64 m/s causes a decrease in the velocity in the centre of the freeboard and increases the velocity in the vicinity of the walls in the freeboard. However, when the jet velocity is increased further to 8.64 m/s this trend is reversed such that, compared to the case of a jet velocity of 5.64 m/s, the velocity in the centre of the freeboard is higher, while the velocity near the walls is decreased.

Discussion

The simulated bubble eruption pattern shown in Fig. 4 is in qualitative agreement with the experimental measurements of Müller *et al*. [11], given in Figs. 1(b,c), *i.e.* the velocity of the gas released during the bubble eruption process is fairly constant along the dome of the erupting bubble. According to Hartung *et al*. [12], the homogeneous release of gas at the dome of an erupting bubble is one of five possible eruption patterns. However, it has to be mentioned that the pattern in which most of the gas escapes at the outer margins of the dome upon its collapse has been identified as the most common by Hartung *et al*. [12]. An important feature of the bubble eruption model of Levy and Lockwood [8] and Solimene *et al*. [9] is the formation of a toroidal vortex upon dome collapse. It was proposed that the falling particles cause a reversal of the flow of the surrounding gas, which induces the formation of a toroidal vortex, moving initially towards the walls. The formation of a toroidal vortex could not be observed in the DEM simulations. Currently, we cannot give a confident explanation why we do not see a toroidal vortex, however, we believe that the fact that our simulations were (i) 2D while the experimental measurements were 3D and (ii) that the fluidized particles differed in size, *i.e.* 1.2 mm compared to 150 – 250 μm in the experimental measurements may have contributed to the observed differences. For example, it is known that if a stream of bubbles is injected into a bed of large particles, a higher rate of gas leakage into the particulate phase is observed than for bubbles injected into a bed of small particles [18]. The higher rate of gas leakage in beds of larger particles may, thus, also influence the release of gas from an erupting bubble.

Turning now to the time-averaged gas velocity measurements, Fig. 5(a) demonstrates convincingly that the vertical velocity in the freeboard of a fluidized bed which is held at minimum fluidization and into which a stream of bubbles is released, is lowest in the centre of the bed and highest in the vicinity of the walls. Such gas characteristics have been observed experimentally by Duursma *et al*. [13] and Müller *et al*. [11]. The only difference, between the numerical and experimental studies is the fact that in the numerical studies the vertical velocity in the centre of the fluidized bed is directed upwards, whereas in experimental studies the time-averaged vertical velocity is negative, *i.e.* directed downwards. Again, we can

only speculate as to the reason for this discrepancy is and suspect that the differences in (i) geometry (2D versus 3D) and (ii) particle size are the main reasons for the observed difference. We are currently performing simulations with smaller particles unequivocally to answer the question of how the particle size influences the gas dynamics in the freeboard.

When the jet velocity is increased from 3.64 m/s to 5.64 m/s, the vertical velocity in the centre of the freeboard decreases, which is in agreement with the experimental measurements of Müller *et al*. [11]. When the gas velocity is further increased to 8.64 m/s, however, the velocity in the centre of the freeboard increases again. One explanation for this behaviour may be that the erupting bubbles direct gas towards the walls causing a decrease in the velocity in the centre of the freeboard and an increase in the velocity near the walls. Increasing the jet velocity from 3.64 m/s to 5.64 m/s increases the bubble frequency, causing more gas to be diverted towards the sidewalls. The reversal in the trend when the jet velocity is 8.64 m/s may be due to the stronger jet forcing more gas through the centre of the bed, or may be due to a change in the nature of the bubbles, which become larger as the jet velocity is increased.

Another interesting feature of gas flow in a fluidized bed, *i.e.* the gas flow through a rising bubbles, was well simulated with the DEM. Figure 3(b) shows the gas uses the rising bubble as a low pressure-drop short cut. Such a gas velocity profile is expected for slow bubbles, *i.e*. for bubbles whose rise velocity U_b is less than the interstitial minimum fluidization velocity [18]. For the bubble shown in Fig. 3(b), the bubble rise velocity was determined as 0.55 m/s, whereas the interstitial minimum fluidization velocity was 1.68 m/s, *i.e*. the bubble is a slowly rising bubble.

Conclusions

Discrete Element Model (DEM) simulations were used to study the eruption patterns of bubbles and the gas velocity profile in the freeboard of a fluidized bed which was held at minimum fluidization and a continuous stream of bubbles was released through a central orifice. The results of the numerical simulations were compared to experimental Particle Image Velocimetry (PIV) and acetone planar laser induced fluorescence (PLIF) measurements of Müller *et al*. [11]. In the DEM simulations the velocity of the gas leaving an erupting bubble was homogeneously distributed along the bubble dome, one of five possible eruption patterns reported by Hartung et al. [12]. The time-averaged gas velocity profile revealed that, in the freeboard, the lowest velocity in the vertical direction was in the centre of the bed, whereas the highest was in vicinity to the walls, in agreement with results reported by Duursma *et al*. [13] and Müller *et al*. [11]. However, unlike in experimental measurements, the vertical velocity of the gas was still directed upwards in the centre of the freeboard.

References

[1] Scott, S. A., Davidson, J. F., Dennis, J. S., Hayhurst, A. N, "The devolatilisation of particles of a complex fuel (dried sewage sludge) in a fluidise bed", *Chem. Eng. Sci.* 62: 584–598 (2007).

[2] Solimene R, Marzocchella A, Ragucci R, Salatino P,. "Flow structure and gas-mixing induced by bubble bursting at the surface of an incipiently gas-fluidized bed", *Ind Eng Chem Res*.43: 5738–5753 (2004).

[3] Li, J. L.; Kato, K. "A correlation of the elutriation rate constant for adhesive particles (group C particles)", *Powder Technol.* 118: 209–218 (2001).

[4] Santana, D.; Rodriguez, J.; Macias-Machin, A. "Modelling fluidized bed elutriation of fine particles", *Powder Technol.* 106*:* 110–118 (1999).

[5] Choi, J. H.; Suh, J. M.; Chang, I. Y.; Shun, D. W.; Son, J. E.; Kim, S. D. "The effect of fine particles on elutriation of coarse particles in a gas fluidized bed", *Powder Technol.* 26: 190–194 (2001).
[6] Zenz, F. A.; Weil, N. A. "A theoretical-empirical approach to the mechanism of particle entrainment from fluidized beds",*AIChE J.* 4*:* 472–479 (1958).
[7] Pemberton ST, Davidson JF. "Elutriation from fluidized beds -1. Particle ejection from the dense phase into the freeboard", *Chem Eng Sci*. 41: 243–251 (1986).
[8] Levy, Y.; Lockwood, F. C. Laser doppler measurements of flow in freeboard of a fluidized bed. *AIChE J.* 29: 889–895 (1983).
[9] Solimene, R.; Marzocchella, A.; Ragucci, R.; Salatino, P., "Laser diagnostics of hydrodynamics and gas-mixing induced by bubble bursting at the surface of gas-fluidized beds", *Chem. Eng. Sci.* 62*:* 94–108 (2007).
[10] Yorquez-Ramirez MI, Duursma GR., « Insights into the instantaneous freeboard flow above a bubbling fluidized bed", *Powder Technol*. 116: 76–84 (2001).
[11] Müller, C.R., Hartung, G., Hult, J., Dennis, J.S., Kaminski, C.K., "Laser Diagnostic Investigation of the Bubble Eruption Patterns in the Freeboard of Fluidized Beds: Simultaneous Acetone PLIF and Stereoscopic PIV Measurements", *AIChE J*. 55: 1369-1382 (2009).
[12] Hartung, G., Müller, C.R., Hult, J., Dennis, J.S., Kaminski, C.K., "Laser Diagnostic Investigation of the Bubble Eruption Patterns in the Freeboard of Fluidized Beds. 1. Optimization of Acetone Planar Laser Induced Fluorescence Measurements", *Ind. Eng. Chem. Res*. 47: 5686-5697 (2008).
[13] Duursma GR, Glass DH, Rix SJL. Yorquez-Ramirez M.I, "PIV investigations of flow structures in the fluidized bed freeboard region", *Powder Technol*. 120: 2–11 (2001).
[14] Tsuji, Y., Kawaguchi, T. Tanaka, T., "Discrete particle simulations of 2-dimensional fluidized-beds", *Powder Technol*. 77: 79–87 (1993).
[15] Cundall, P.A., Strack, C.D.L., "Discrete numerical-model for granular assemblies", *Geotechnique* 29: 47–65 (1979).
[16] Anderson, T.B., Jackson, R., "A fluid mechanical description of fluidized beds", Ind. & Eng. Chem. Fund. 6: 527–539 (1967).
[17] Beetstra, R., van der Hoef, M.A., Kuipers, J.A.M., "Numerical study of segregations using a new drag force correlation for polydisperse systems derived from lattice-Boltzmann simulations", *Chem. Eng. Sci*. 62: 246–255 (2007).
[18] Davidson, J.F., Harrison, D., *Fluidised Particles*, Cambridge University Press, 1963.